XV International Conference on Durability of Building Materials and Components
DBMC 2020, Barcelona
C. Serrat, J.R. Casas and V. Gibert (Eds)

A Probabilistic Model for the Evolution of Porous Structure Caused by Solid-Phase Precipitation/Dissolution within Building Materials

Xiong Qing Xiang[1, a] and Meftah Fekri[1, b]

[1]Laboratory of Civil and Mechanical Engineering (LGCGM), National Institute for Applied Sciences, Campus Beaulieu, 35700 Rennes, France
[a]qingxiang.xiong@insa-rennes.fr, [b]fekri.meftah@insa-rennes.fr

Abstract. *Saline intrusion is a critical issue in building material because of the severe damages caused by the salt precipitation/dissolution process, especially for the porous material, which has good connectivity. When porous material is exposed to aggressive ambient, the pore structure, not only porosity but also pore size distribution, will be altered by salt precipitation/dissolution. As one of the most significant characteristics in the porous material, pore size distribution is always paid much attention in many literatures. However, a quantitative and practical determination method is still absent. This work aims to establish a probabilistic model to investigate the pore size distribution induced by solid-phase precipitation/dissolution. First, a lognormal distribution is proposed for the simulation of initial pore size distribution tested by the MIP method. Then we develop a probabilistic-based porous network to represent the evolution of microstructure due to precipitation/dissolution. To this end, two different transformation models are constructed to interpret the relation between initial pore radius and modified pore radius before and after precipitation/dissolution. With this probabilistic-based porous network, we could illustrate the precipitated profiles that evolve near the capillary interface during the salt precipitation/dissolution process for a given porosity and water saturation degree. Such a method could be used to interpret the mechanism of the local precipitation/dissolution process in pore scales, which cannot be implemented by experimental measurements.*

Keywords: *Pore Size Distribution, Precipitation/dissolution, Capillary Interface, Probabilistic Methods, Transformation Models.*

1 Introduction

The durability of construction material is always prevalently focused research since it is strictly relevant to the long and durable service life of building structures. As is generally accepted, salt precipitation/dissolution is one of the main factors for the deterioration of construction material, especially for the porous construction material, which has highly connected cavity facilitating the transport of moisture, ions, and chemical fluxes (Huang *et al.,* 2015). Salt precipitation/dissolution strongly influences the pore structure, which governs the most important properties of porous material, notably compressive strength for cement-based media (Cristina *et al.,* 2012). For example, salt dissolution induces high porosity, which accelerates the permeability of gases and liquids within the pore structure, thus affects the compatibility and durability of the construction materials. As a result, it brings about high maintenance and repair costs. (Fenaux *et al.,* 2019; Kumar *et al.,* 2003). Therefore, the porous structure directly impacts the durability and resistance of construction material and components. More specifically speaking, research on the processes involved in salt-induced corrosion is of utmost benefit for assessing the durability of construction material.

Apart from the porosity, the pore size distribution (PSD) also plays a vital role in

characterizing pore structure within porous media (Aligizaki *et al.,* 2005). However, the porosity does not give any information about pore size, shape, distribution, and connectivity; thus, the PSD should be employed to give a precise depiction of pore structure. The PSD, which is so complicated that covers several orders of magnitude of pore size, is principally influenced by several aspects, for instance, water, air, chemical reactions, and other fluids. (JR Nimmo, 2013) It is essential to recognize that many efforts of experimental measurements have been devoted to the description of PSD by previous researchers (D.N. Winslow, 1968; S. Roels *et al.,* 2001; E.Gallucci *et al.,* 2007; Yanbin Yao *et al.,* 2012; Gong Fuyuan *et al.,* 2014). However, a quantitative and practical determination method is still absent. Since the pore structure is heterogeneous and anomalous morphology in pore sizes, it is hard to describe it in full detail by experimental measurements. Therefore, the most reasonable method is to assess it by probabilistic models.

In this work, we adopted a lognormal distribution to approach the initial PSD before solid-phase precipitation occurred. Two representative models for pore radius were constructed by employing a monotonic transformation model and a non-monotonic transformation model. After several times of solid-phase precipitation, the new PSD was described by two different probabilistic methods. According to the comparison and parametric investigations, the proposed methods could provide us with an estimated prediction of the modified PSD, filling rate, and water saturation degree.

2 Methodologies

2.1 Transformation Models for Pore Radius

During the process of solid-phase precipitation/dissolution, the initial pore radius goes through a multi-step of transformation with the evolution $r_0 \to r_1 \to \cdots \to r_n \to r_{n+1}$, which is corresponding to the evolution of total porosity $\phi_0 \to \phi_1 \to \cdots \to \phi_n \to \phi_{n+1}$. According to the superposition principle, the new pore radius $r_{n+1}$is the superimposed of the current pore radius r_n and the increment term denoted as $\varepsilon_{n+1}(r_n)$, which is expressed as equation (1). As is mentioned above, precipitation/dissolution occurs near the capillary interface. Thus, the waterfront r_c is introduced into the transformation models of the pore radius. For the sake of simplification, it is assumed that the waterfront keeps constant as the evolution of pore structure. That is to say, the proposed pore system is open to the atmosphere to induce the water to evaporate into the ambient, which makes the waterfront be equilibrium. In this way, the capillary interface keeps constant for each time of transformation.

$$r_{n+1} = f_{n+1}(r_n) = r_n + \varepsilon_{n+1}(r_n) \tag{1}$$

Let us consider two different cases for the increment function $\varepsilon_{n+1}(r_n)$. For the monotonic model (see Figure 1a), water is filled in all the pores with the radius less than r_c. Solid-phase condenses inside the pores with the radius ranging from $r_c - \beta$ to $r_c + \beta$. When pore radius is large enough (*i.e.,* more than $r_c + \beta$), the accumulated solid-phase is assumed to be constant as $\bar{\varepsilon}_{n+1}$. For the non-monotonic model (see Figure 1b), the precipitated solid only occurs near the waterfront with the range from$r_c - \beta$ to $r_c + \beta$; for large pores with radius more than $r_c + \beta$, solid mass is supposed to be small enough to be neglected when compared to the large pore space.

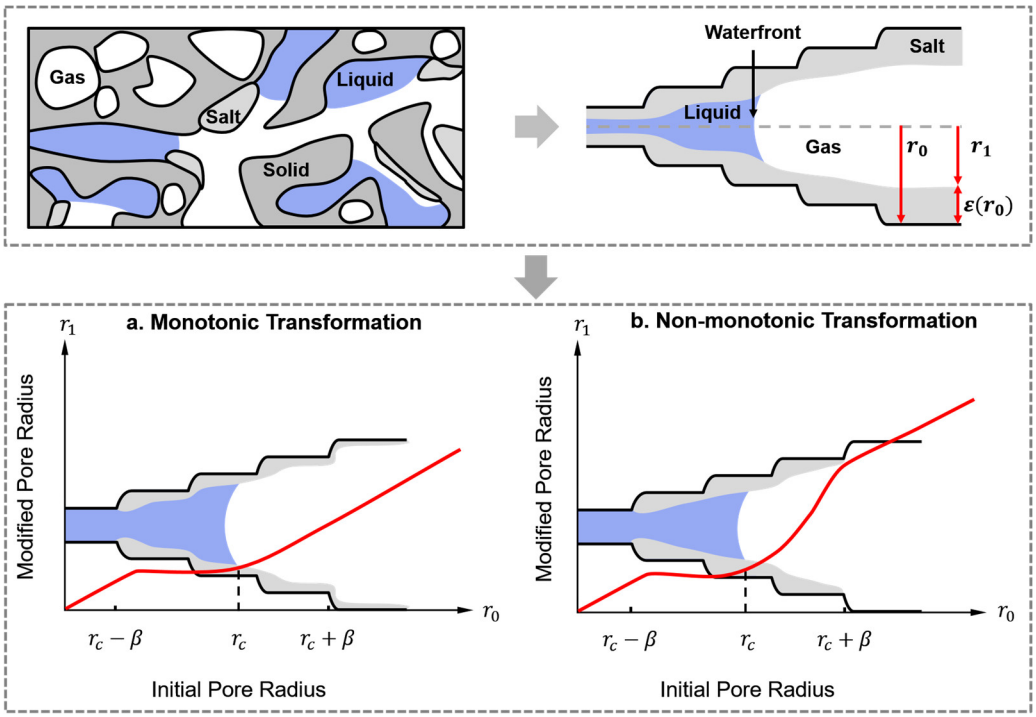

Figure 1. Schematic of the porous model for one single transformation (r_c is the maximum aperture filled with water, the so-called waterfront or capillary interface; β is the opening zone, indicating the range of solid precipitation/dissolution, $\varepsilon(r_0)$ is the increment term for the first time of transformation.).

Table 1. The monotonic transformation model and non-monotonic transformation model for new pore radius.

Function	Monotonic transformation model	Non-monotonic transformation model
$\varepsilon_{n+1}(r_n)$	$\begin{cases} 0 & r_n < r_c-\beta \\ \bar{\varepsilon}_{n+1}H(r_n) & r_c-\beta \le r_n \le r_c+\beta \\ \bar{\varepsilon}_{n+1} & r_n > r_c+\beta \end{cases}$	$\begin{cases} 0 & r_n < r_c-\beta \\ \bar{\varepsilon}_{n+1}H(r_n) & r_c-\beta \le r_n \le r_c \\ \bar{\varepsilon}_{n+1}G(r_n) & r_c \le r_n \le r_c+\beta \\ 0 & r_n > r_c+\beta \end{cases}$
$H(r_n)$	$\frac{3}{4}\left(\frac{r_n-r_c}{\beta}-\frac{(r_n-r_c)^3}{3\beta^3}\right)+\frac{1}{2}$	$\frac{3}{4}\left(\frac{2r_n+\beta-2r_c}{\beta}-\frac{(2r_n+\beta-2r_c)^3}{3\beta^3}\right)+\frac{1}{2}$
$G(r_n)$		$-\frac{3}{4}\left(\frac{2r_n-\beta-2r_c}{\beta}-\frac{(2r_n-\beta-2r_c)^3}{3\beta^3}\right)+\frac{1}{2}$
Remarks	The derived function should satisfy $H'(r_n) > 0$ in the case of salt precipitation, that is, $\bar{\varepsilon}_{n+1}$ is constrained in the range of $[0, -4/3\beta]$	

Table 1 shows the details of two different transformation functions. It should be noted if parameter $\bar{\varepsilon}_{n+1} > 0$, salt dissolution occurs; if $\bar{\varepsilon}_{n+1} < 0$, salt precipitation occurs. For the monotonic transformation model, the derived function $H'(r_n)$ should be positive to make sure the transformation function is one-to-one.

2.2 Probabilistic Methods for Modified Pore Size Distribution

The initial PSD for gel pores and capillary pores is presented in the form of lognormal probability density function that is expressed as:

$$P_0(r_0) = \frac{1}{\sigma_r\sqrt{2\pi}\, r_0} \exp\left(-\frac{(\ln r_0 - \mu_r)^2}{2\sigma_r^2}\right) \tag{2}$$

where μ_r, the location parameter, is the arithmetic mean of the representative pore size and σ_r, the standard deviation, is a measure of the dispersion of these pore size.

The total porosity for n+1th transformation is defined as:

$$\phi_{n+1}(r_{n+1}) = \phi_{n+1} \int_0^{r_{n+1}} P_{n+1}(t)dt \tag{3}$$

As we have the initial PDF $P_0(r_0)$ and two transformation models for pore radius, the new probability density function $P_{n+1}(r_{n+1})$ for n+1th transformation could be determined by the following two methods, which are presented in Table 2.

Table 2. Two probabilistic methods and their properties.

	Method one	Method two
Theoretical foundation	It is based on the assumption that porosity is proportionally distributed to each pore, the ratio of local porosity before and after transformation is equal to that of the ratio of global porosity: $\frac{\phi_{n+1}}{\phi_n} = \frac{d\phi_{n+1}}{d\phi_n}$	Let us consider the cylindrical form of the pores as to the end that the ratio of local porosity before and after transformation is equal to the ratio of pore volume, which could be represented by the following equation: $\frac{d\phi_{n+1}}{d\phi_n} = \frac{r_{n+1}dr_{n+1}}{r_n dr_n}$
P_{n+1}	$\left\lvert\left(\frac{dr_{n+1}(r_n)}{dr_n}\right)^{-1}\right\rvert P_n(r_n)$	$\frac{\phi_n}{\phi_{n+1}}\frac{r_{n+1}(r_n)}{r_n}P_n(r_n)$

According to Figure 1, the capillary condensation occurs in pores with radii smaller than r_c, thus the water saturation degree S_l (SD) can be obtained by the integration of the volume pores with sizes smaller than r_c.

$$S_l = \int_0^{r_c} P_{n+1}dr_n \tag{4}$$

3 Implementation and Parametric Study

The inputs parameters of initial pore size distribution were completed by experimental test mercury intrusion porosimetry (MIP) on masonry cement (see in Table 3 for more properties).

As the limitation of space, only the process of solid precipitation ($\bar{\varepsilon}_{n+1} < 0$) will be discussed in this work. The waterfront could occur in any position of capillary pores, ranging from 0.0025μm to 5μm (Huang et al., 2015), thus, the opening zone β could be any value that

is smaller than r_c.

Table 3. Characteristic parameters of lognormal distribution for the initial pore radius.

Initial porosity ϕ_0	Standard deviation σ_r	Mean Value μ_r	r_{min} (μm)	r_{max} (μm)
0.20	1.2	-1.8788	0.0015	165

3.1 One Transformation for the Monotonic Model

Let us study one monotonic transformation of PSD evolves with four different capillary interfaces both by method one and method two. When solid-phase precipitation occurs, the porosity is assumed to decrease from 0.2 to 0.18, and the opening zone is fixed at 0.05μm. Then we can get the new PSD for the single transformation according to the equations in Table 1 and Table 2.

Figure 2 indicates that significant and sharp salt precipitation occurs near the waterfront for method one (see in Figure 2a). For method two (see in Figure 2b), the variation of pore radius is much smoother than method one. Moreover, the modification was distributed evenly to the whole range of pore size in method two. Thus, it can be concluded that for the porous materials sensitive to the capillary effect, such as the porous material with a large number of fine pores and high permeability, method one is more appropriate to describe the slight salt deposition process than method two. Of course, the extent of salt precipitation also depends on the type of salts, temperature, concentration, and saturation degree of salt solution.

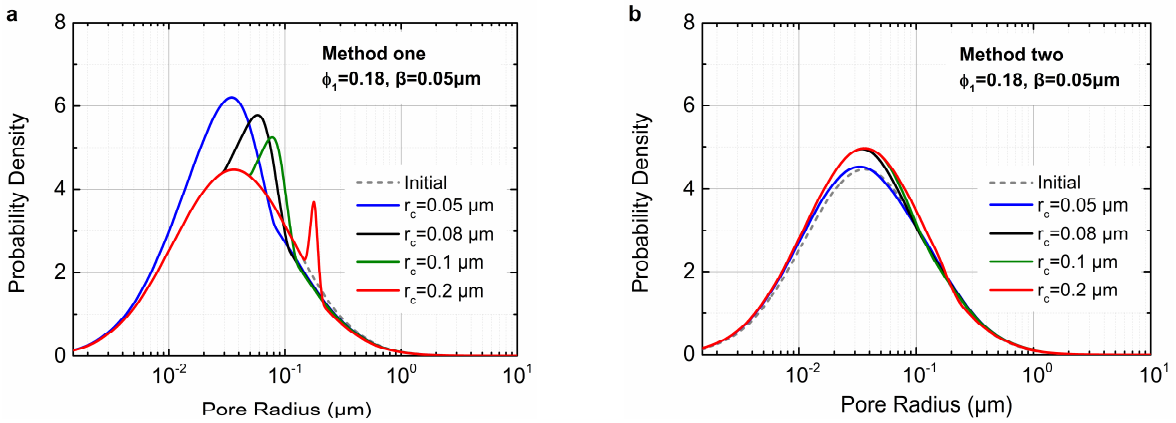

Figure 2. Pore size distribution with different waterfront for single transformation.

3.2 Successive Transformations for the Non-Monotonic Model

For the case of non-monotonic transformation models, we focus on five times of successive transformations with the porosity decreasing from 0.20 to 0.18 in the step of 0.004. The waterfront is fixed at 0.1 μm, and the opening zone is valued at 0.08μm. For non-monotonic transformation, there is no constraint to new porosity, and all we should concern about is that the critical parameter $\bar{\varepsilon}_{n+1}$cannot make the new pore radius negative.

From Figure 3, we can find that both method one and method two generate a bimodal probability density as the porosity decreasing to a specific value. As is similar to the single transformation, the probability density presented by method one shows a noticeable increment

of the peak value. In contrast, the probability density curve implemented by method two shows a slight shift to the left side, indicating produced more fine pores with the effect of precipitation.

As to the filling rate of pore radius due to the solid-phase precipitation presented in Figure 4, by dividing $\varepsilon_{n+1}(r_0)$ with r_0, after one time of transformation, that of the method one is up to 30% while that of the method two accomplishes around 10%. After five times of transformation, when the porosity decreases to 0.18, the porous material described by method one has the filling rate of almost reaching 70%, while method two only achieves over 30%. Thus, at the same porosity, method one presents a more efficient filling rate of pore radius than method two.

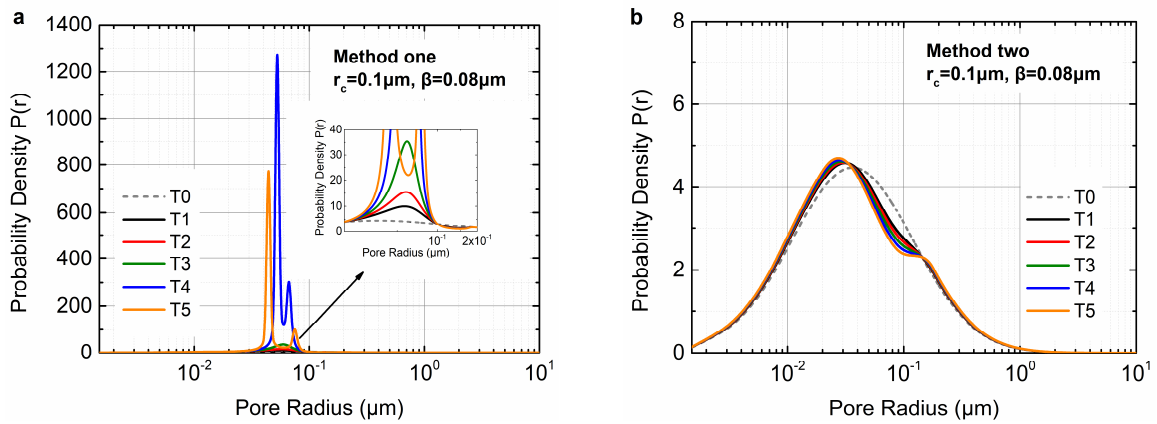

Figure 3. Pore size distribution for successive non-monotonic transformations by two different methods (According to Table 2, method one is related to the reciprocal of the derivative function of the non-monotonic transformation model, which induces the singularity points at the positions where the derivative function is equal to zero. As a result, the PDF tends to infinity at these singularity points. Herein the unbounded PDF is allowed because the integral of the modified PDF from 0 to ∞ is equal to 1.).

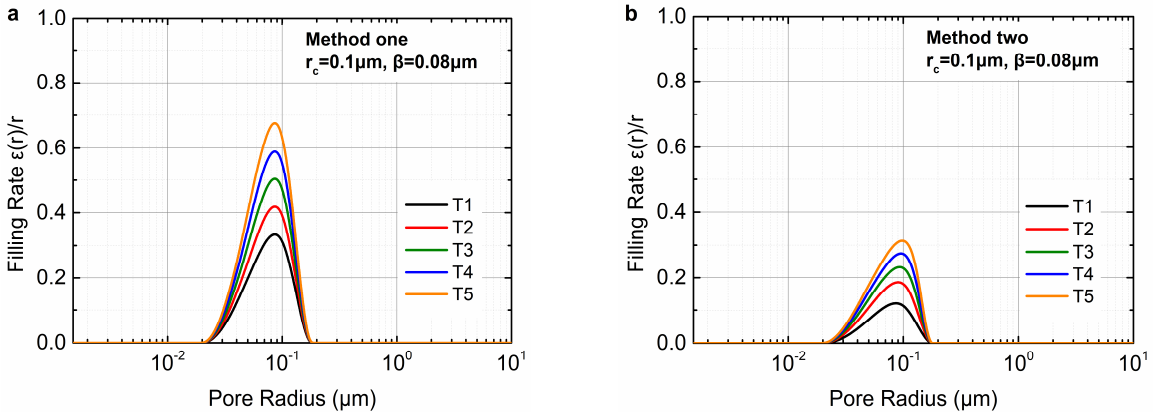

Figure 4. Filling rate of pore radius by two different methods during the process of salt precipitation.

To investigate the evolution of water saturation degree for successive transformations, we consider a case that porosity decreases from 0.2 to 0.185 by 30 steps, as is shown in Table 4.

Table 4. Parameter configurations for the investigation of the water saturation degree in non-monotonic successive transformations.

Initial porosity ϕ_0	Final porosity ϕ_{30}	Transformation Times	Transformation Steps of Porosity	Waterfront r_c (μm)	Opening Zone β (μm)
0.2	0.185	30	0.0005	0.1	0.08

Figure 5 shows the evolution of the water saturation degree with the porosity. It is observed that the water saturation degree calculated by method one shows a slight reduction while that is described by method two increases tremendously with the porosity decreasing. Besides, the incremental trend is more and more evident as the decreased porosity. It may be ascribed to the different filling rates of the two methods. For method two, the reduction rate of the pore volume is lower than that of water volume, leading to the increment of the water saturation degree. However, for method one, the reduction rate of the pore volume is fast enough to catch that of the water volume, and the two rates are almost the same. Consequently, the water saturation degree by method two almost keeps constant.

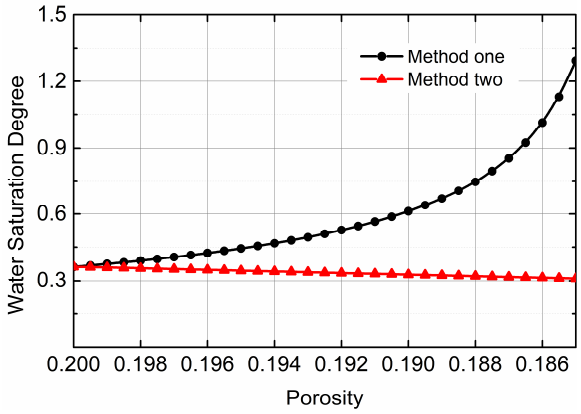

Figure 5. Water saturation degree implemented by two methods in the case of salt precipitation.

4 Conclusions

- When the waterfront moves to large pores, method one shows more evident modification than method two for PSD in the process of salt precipitation. Moreover, method one is more appropriate to the porous material that is sensitive to the capillary effect than method two. Besides, the monotonic model is very limited used, which is only applicable to the slight salt precipitation.
- The existing two probabilistic methods could estimate the filling rate caused by salt precipitation. According to the simulated results of non-monotonic transformation models after five times of transformations, method one has a higher filling rate than method two, which indirectly leads to the stable water saturation degree in method one. Such an approach of method one allows the water condensation in the open system that does not depend on the evolution of the pore structure.
- For further investigation, proper consideration for the mobilization of waterfront in a closed system should be taken into account to fully understand the evolution of

microstructure in the durability research for a porous material.

Acknowledgement

The author acknowledges Professor Ouali. Amiri of his generous providing experimental tested results for the reference of our work.

ORCID

Amiri, O: https://doi.org/10.1680/adcr.2005.17.1.39
Baroghel-Bouny Véronique: https://doi.org/10.1016/j.cemconres.2006.11.019
Fenaux, M : https://doi.org/10.1016/j.cemconcomp.2018.12.009
Gallucci Emmanuel: https://doi.org/10.1016/j.cemconres.2006.10.012
Gentilini Cristina : https://doi.org/10.1016/j.conbuildmat.2012.07.086
Gong Fuyuan: https://doi.org/10.1061/(ASCE)MT.1943-5533.0000945
Huang Qinghua: https://doi.org/10.1016/j.cemconres.2014.08.003
Kumar Rakesh: https://doi.org/10.1016/S0008-8846(02)00942-0
Nimmo, J: https://doi.org/10.1016/B978-0-12-409548-9.05265-9
Roels Staf: https://doi.org/10.1007/BF02481555
Windslow, D.N: https://doi.org/10.5703/1288284313747
YanbinYao: https://doi.org/10.1016/j.fuel.2011.12.039

References

Amiri, O., Aït-Mokhtar, A. and Sarhani, M. (2005). Tri-dimensional modelling of cementitious materials permeability from polymodal pore size distribution obtained by mercury intrusion porosimetry tests. Advances in Cement Research, 17(1), 39–45.

Aligizaki, K. K. (2005). Pore Structure of Cement-Based Materials: Testing, Interpretation and Requirements. CRC Press.

Fenaux, M., Reyes, E., Gálvez, J. C. and Moragues, A. (2019). Modelling the transport of chloride and other ions in cement-based materials. Cement and Concrete Composites, 97, 33–42.

Gallucci, E., Scrivener, K., Groso, A., Stampanoni, M. and Margaritondo, G. (2007). 3D Experimental Investigation of the Microstructure of Cement Paste Using Synchrotron X-Ray Microtomography (mu CT). Cement and Concrete Research, 37, 360–368.

Gentilini, C., Franzoni, E., Bandini, S. and Nobile, L. (2012). Effect of salt crystallisation on the shear behaviour of masonry walls: An experimental study. Construction and Building Materials, 37, 181–189.

Gong Fuyuan, Zhang Dawei, Sicat Evdon, and Ueda Tamon. (2014). Empirical Estimation of Pore Size Distribution in Cement, Mortar, and Concrete. Journal of Materials in Civil Engineering, 26(7), 04014023.

Huang, Q., Jiang, Z., Gu, X., Zhang, W. and Guo, B. (2015). Numerical simulation of moisture transport in concrete based on a pore size distribution model. Cement and Concrete Research, 67, 31–43.

Kumar, R. and Bhattacharjee, B. (2003). Porosity, pore size distribution and in situ strength of concrete. Cement and Concrete Research, 33(1), 155–164.

Nimmo, J. (2013). Porosity and Pore Size Distribution. Reference Module in Earth Systems and Environmental Sciences.

Roels, S., Elsen, J., Carmeliet, J. and Hens, H. (2001). Characterisation of pore structure by combining mercury porosimetry and micrography. Materials and Structures, 34(2), 76–82.

Windslow, D.N. (1968). The Pore Size Distribution of Portland Cement Paste. JTRP Technical Reports.

Yao, Y. and Liu, D. (2012). Comparison of low-field NMR and mercury intrusion porosimetry in characterizing pore size distributions of coals. Fuel, 95, 152–158.